Resonant Crossover of Terahertz Loss to the Gain of a Bloch Oscillating InAs/AlSb Superlattice

P. G. Savvidis,[1] B. Kolasa,[1] G. Lee,[2] and S. J. Allen[1,*]

[1]*Center for Terahertz Science and Technology, University of California, Santa Barbara, California 93106, USA*
[2]*Agilent Laboratories, 3500 Deer Creek Road, Palo Alto, California 94304-1317, USA*

(Received 14 November 2003; published 13 May 2004)

Terahertz absorption in waveguides loaded with InAs/AlSb super-superlattice mesas reveals a frequency dependent crossover from loss to gain that is related to the Stark ladder produced by an applied dc electric field. Electric field domains appear to be suppressed in the super-superlattice composed of many very short segments of superlattice, interrupted by heavily doped InAs regions. Resonant crossover is indicated by an increase in terahertz transmission as the Stark splitting or Bloch frequency determined by the applied dc electric field exceeds the measurement frequency.

DOI: 10.1103/PhysRevLett.92.196802 PACS numbers: 73.50.Mx, 07.57.Hm, 72.20.–i, 73.21.Cd

Bloch oscillation was theoretically recognized as a fundamental aspect of electrical transport in periodic structures more than 70 years ago [1], but only recently have aspects of Bloch oscillation been experimentally uncovered in two quite different systems. Key experiments in semiconductor superlattices have shown Wannier-Stark ladders [2,3], transient Bloch oscillations [4–7], and resonant terahertz photoconductivity [8]. The most elegant and graphic experiments on Bloch oscillation and Zener tunneling appear in cold atoms in optical periodic potentials [9–11].

The seminal work of Esaki and Tsu [12] drew attention to the fact that the relatively large scale periodic structures in semiconductor superlattices made them ideal solids in which to explore and use Bloch oscillation. While they focused on bulk dc negative dynamical conductance, Ktitorov *et al.* developed a semiclassical treatment [13] of its frequency dependence which they showed can persist up to the Bloch frequency; above the Bloch frequency or the equivalent Stark ladder splitting, the material becomes lossy [7,14]. More recently Willenberg *et al.* [15] showed theoretically that the Ktitorov result was valid over a wide range of superlattice parameters and electrical biases. From this perspective an electrically biased superlattice is a gain medium with high frequency cutoff at the Bloch frequency. Since the applied voltage can control the Bloch frequency, it has the potential to be the basis of a very high frequency, perhaps terahertz frequency, solid state source.

Figure 1(a) displays a Stark ladder caused by the application of a uniform electric field across a relatively short section of superlattice. The spacing between rungs of the ladder is eEd and equal to $\hbar\omega_B$, where ω_B is the Bloch frequency. Semiclassically, electrons undergo *incoherent* oscillatory motion at frequency ω_B and are restricted to a spatial region $\sim\Delta/eE$ (Δ is the miniband width and E is the applied electric field). Electrons undergoing Bloch oscillation do not contribute to the dc current, suppressing the net current leading to negative dynamical conductance (NDC).

Figure 1(c) displays the real part of the dynamical conductance, dI/dV, following Ktitorov *et al.* [13] and assuming equal elastic and inelastic scattering times of $\tau \sim 0.095$ ps. At dc the dynamical conductance is suppressed and eventually becomes negative when $\omega_B\tau > 1$. However, at high frequency the suppression is predicted to develop more gradually and the dynamical conductance becomes negative only when the Bloch frequency exceeds the measurement frequency.

With these theoretical models we can set aside the naive view of a "Bloch oscillator." A Bloch oscillator does not simply oscillate at the Bloch frequency; it

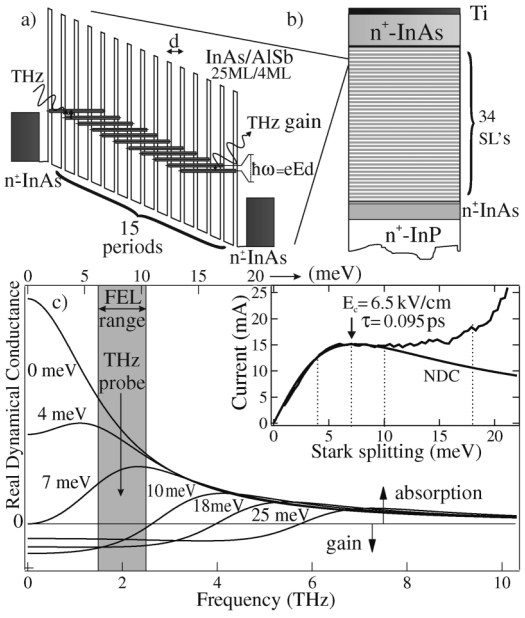

FIG. 1. (a) The superlattice structure under dc bias sandwiched between two n^+ regions. (b) Super-superlattice mesa structure is a repetition of 34 cells depicted in (a). (c) Real dynamical conductance, dI/dV, versus frequency for different applied electric fields using scattering parameters consistent with the dc I-V shown in the inset. Electric fields are given in units of the energy spacing of the Stark ladder states.

oscillates at a frequency controlled by the external resonator or circuit but only at frequencies below the Bloch frequency. That said, the frequency dependent crossover from negative to positive dynamical conductance is fundamental to the concept of Bloch oscillating superlattices and their potential use in very high frequency solid state sources.

We report here measurements of the crossover from loss to gain, at terahertz frequencies in an electrically biased semiconductor superlattice [16] by measuring the dynamical conductance at selected terahertz frequencies in the band in Fig. 1(c); we take a vertical cut through Fig. 1(c). Experiments were carried out at room temperature.

While the Stark ladder in Fig. 1(a) invokes the concept of the quantum cascade laser that has been successfully made to operate at frequencies below 3 THz [17–19], there is an essential difference. The gain appears without net population inversion between the rungs of the Stark ladder. Shedding the requirement of population inversion may make this system more attractive as a room temperature device at lower frequencies.

However, it is well known that a medium with bulk NDC exhibits space charge instabilities that lead to electric field domains and current self-oscillations [20,21]. But, if the material is sufficiently short, small space charge fluctuations that grow and provide electric field domain walls are swept out before a domain wall is established. As in the Gunn effect, we can define a critical "nL" product below which propagating electric field domains are suppressed. Here, n is the electron density and L is the sample length. For a semiconductor superlattice we estimate that if $nL \lesssim 7\epsilon\epsilon_0 E_c/e$, where ϵ is the dielectric constant and E_c the critical field at which NDC sets in, space charge instabilities are swept out of the superlattice before they form a domain wall [22,23]. The doping density in the superlattices under test was $n \sim 2 \times 10^{16}$ cm^{-3} requiring lengths of the order of 150 nm to mitigate propagating Gunn effect like space charge instabilities.

Armed with this estimate the superlattice material was engineered as a stack of ~150 nm superlattices interrupted by 100 nm of heavily doped material [Figs. 1(a) and 1(b)] to prevent the formation of static or propagating domains. Presumably these heavily doped layers allow carriers to equilibrate and the quantum transport in each short superlattice behaves independently. The results suggest that this approach was reasonably successful.

The super-superlattice structure is grown on an n^+-InP substrate by molecular beam epitaxy [Fig. 1(b)]. A 1 μm thick n^+-InAs buffer layer is grown followed by the 8 μm high super-superlattice structure as a stack of 34, 15 period, InAs/AlSb superlattices separated by a 100 nm thick n^+-InAs layer. One super cell consists of 15 periods of 25 ML wide InAs wells and 4 ML wide AlSb barriers. Unintentional doping leaves a concentration of about $n = 2 \times 10^{16}$ cm^{-3}. The structure is capped by a 2 μm thick layer of n^+-InAs.

The width of the lowest and first excited minibands are calculated to be $\Delta = 50$ and 150 meV, respectively, and separated by about 320 meV [24]. We expect that, at moderate electric fields, the superlattice transport is confined to the lower miniband and Zener tunneling or thermal activation to the second miniband is minimized.

The current-voltage (I-V) characteristic for a 10 μm diameter, dry etched, mesa [Fig. 2(a)] is shown as an inset of Fig. 1(c). The low voltage portion of the I-V characteristic is fit to model calculation of the I-V with equal elastic and inelastic scattering times of the order of 0.095 ps. The voltage scale is the average voltage drop per quantum well, $V/(34 \times 15)$. The rise in the current above 15 meV is attributed to thermal excitation of the carriers into the second miniband due to heating [25].

To conduct THz absorption spectroscopy, two rows of superlattice mesas with 25 μm pitch are loaded into the center of a waveguide (335 μm wide) [Fig. 2(b)]. The bottom of the waveguide is formed by the n^+ substrate. The sidewalls of the waveguide are defined by an array of posts that act like photonic band gap material with a stop band 1.35–2.3 THz. A distributed Bragg reflector (DBR)-like structure is fabricated on either side of the photonic crystal to block any unwanted radiation from propagating through the sides of the waveguide. The top part of the waveguide is formed by gold coated (7000 Å) brass (sub 0.3 μm roughness) and is also used to contact the superlattice mesas. Both DBR and photonic crystal structures are etched 1 μm below the superlattice mesas to avoid electrical contact with the top part of the waveguide.

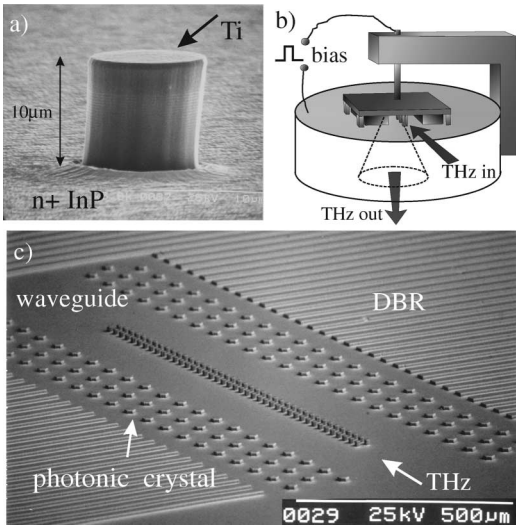

FIG. 2. (a) Super-superlattice mesa. (b) A schematic of the structure in (c) pressed onto the metal surface with a hole to form a waveguide and outcoupling hole. (c) Waveguide without the top metal. A double row of super-superlattice mesas in the middle of the waveguide. Sidewalls are defined by a photonic bandgap structure.

Radiation is collected from the center of the waveguide through a 500 μm size hole in the brass and guided to a fast InSb bolometer [Fig. 2(c)]. Only THz radiation transmitted through the waveguide interacting with the ridge of electrically biased superlattice mesas is collected at the detector.

Terahertz radiation from the UCSB free-electron lasers is directed at the entrance of the 10 μm high waveguide. During the pulse of terahertz radiation, the superlattices are biased with a short electrical pulse. Compare Figs. 3(a) and 3(b). This results in an increase in transmission, Fig. 3(b), as the dynamical conductance is suppressed. The fractional change in transmission is recorded as a function of voltage amplitude and displayed for 1.98 THz in Fig. 3(c). The total voltage is divided by the number of quantum wells, 34×15, and the horizontal axis is the nominal Bloch frequency or Stark splitting assuming the voltage is dropped uniformly over each and every short superlattice section.

Using the model calculation used to generate Fig. 1(c), we have calculated the fractional change in transmission

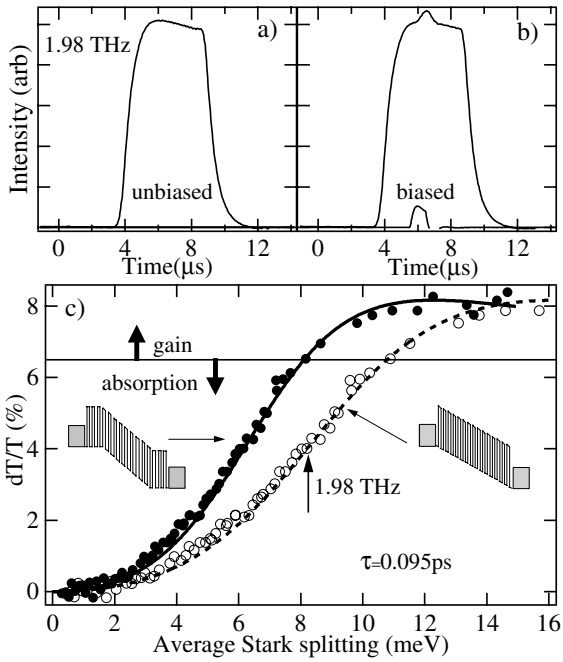

FIG. 3. (a) A pulse of terahertz radiation is transmitted and detected. (b) A short electrical pulse applied to the super-superlattices causes an increase in transmission. (c) Solid circles display the fractional change in transmission as a function of applied voltage displayed as the average voltage drop per quantum well. The predicted dependence based on Fig. 1(c), is shown by the dashed curve. The experimental data can be brought into agreement (open circles) if 0.75 of the quantum wells experience a Stark splitting. The schematic superlattice to the right is uniformly biased; to the left the same voltage drop appears over a fraction of the quantum wells between two n^+ regions. The model indicates that the crossover from loss to gain occurs at different values of the fractional change in transmission.

at 1.98 THz versus Stark splitting and displayed it as a dashed line. (The magnitude is adjusted to fit the maximum measured change of 8%.) The experimental data can be fit well, the solid line, only if one assumes that ~75% of the quantum wells participate in the Stark ladder. There are several possible reasons for this. First, the superlattice is not short enough to completely mitigate electric field domains. Second, the suppression of electric field domains by a short superlattice does not guarantee a perfectly uniform electric field. Third, there is appreciable electron spillover from the heavily doped layers. Nonetheless, we conclude that at this frequency we can quantitatively understand the transmission versus applied voltage if we simply assume that the voltage is dropped across ~75% of the length of each of the superlattices in the structures.

We speculate that if the model used in Fig. 1(c) is correct there is potential gain at 1.98 THz in the structure if the Stark splitting exceeds 8 meV. Note that the critical Stark splitting does not represent a low frequency limit for potential gain. While the system can exhibit no gain until the Stark splitting exceeds 7 meV, gain will occur at low frequencies in sufficiently high electric fields. We cannot know if we have net gain unless the losses are sufficiently low that the system actually amplifies or oscillates.

Figure 4(a) displays similar measurements at six different terahertz frequencies. In each case the data are characterized by an increase in transmission and saturation. If we mark the voltage where the change in transmission achieves 1/2 the maximum value and plot this voltage (average Stark splitting) as a function of the frequency, we discover the linear dependence shown in Fig. 4(b). The crossover depends on the frequency; the higher frequency, the higher voltage or Stark splitting required to sense the suppression of the real dynamical conductance.

To provide a more quantitative measure of the interaction of the terahertz fields with the superlattice loaded waveguide, we have calculated the fractional change in transmission for the first excited even mode depicted in Fig. 4(d). This mode is the first even mode that avoids the lossy ridge. We presume that this mode carries radiation to the detector in the absence of applied dc voltage and the mode that we tune the system to before we excite the superlattices in the ridge with the electrical pulse. The calculated change in transmission, using the model for the dynamical conductance in Fig. 1(c), is shown in Fig. 4(c), at the same terahertz frequencies.

Figure 4(c) appears to reproduce the experimental results in a semiquantitative manner. The magnitude of the fractional change in transmission is very roughly correct, but the systematic increase in $\Delta T/T$ with decreasing frequency is not seen experimentally. At the lower frequencies we are approaching the lower end of the stop band of the photonic band gap sidewall and perhaps the assumed mode profile is incorrect.

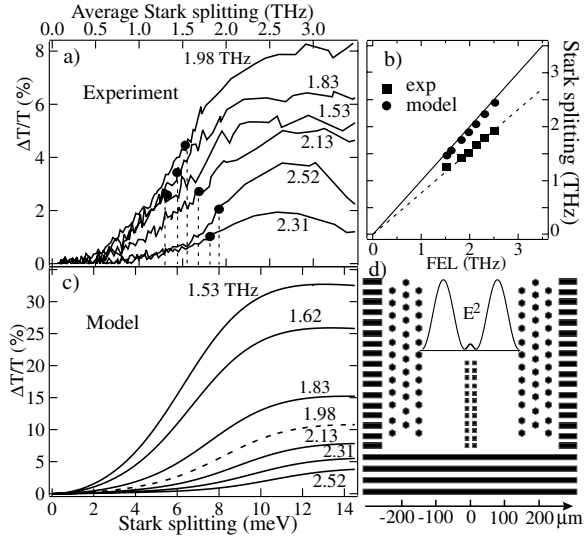

FIG. 4. (a) Experimental fractional change in transmission vs applied voltage for different frequencies. The solid dots indicate the $1/2$ maximum point. This Stark splitting is displayed for different frequencies in (b). The $1/2$ maximum point is a convenient measure to use to compare experiment with the model but the fractional change in transmission that marks the crossover from loss to gain depends on frequency. See Fig. 3(c). (c) Calculated fractional change in transmission vs applied voltage for different frequencies, based on Fig. 1(c). (d) Power density and waveguide schematic.

We can ignore the magnitude of the transmission change in Fig. 4(c) and extract the voltage at which the model predicts the change in $\Delta T/T$ to be $1/2$ the maximum value. We display this voltage versus frequency in Fig. 4(b). The voltage at the $1/2$ maximum point appears to precisely describe the coincidence of the terahertz frequency and the Stark splitting or Bloch frequency but not the precise crossover from loss to gain. As in Fig. 3(c), agreement requires the voltage to be impressed over $\sim$75% of the superlattice material.

In summary, we have measured the terahertz absorption of semiconductor superlattices as a functionof applied voltage. The strong suppression of the loss occurs at an applied electric field that depends on the terahertz frequency confirming the semiclassical predictions of the dynamical conductance. The threshold voltage for suppression of the loss appears to be $\sim$75% of the predicted value implying that the dc field appears over $\sim$75% of the superlattice material. We conclude that fabrication of a super-superlattice, a superlattice consisting of short sections interrupted by heavily doped regions has been largely successful in mitigating dynamic or static electric field domains. The semiquantitative agreement with the predictions of the theoretical model implies that the suppression of loss leads to terahertz gain. We speculate that an electrically biased super-superlattice like that explored here may provide enough gain to fabricate a room temperature terahertz oscillator. Real net gain can be demonstrated only in an amplifier or oscillator. Experiments in this direction continue.

The authors thank Peter Robrish and Rick Trutna, Agilent, for useful discussions. P. S. enthusiastically acknowledges discussions with Ed Ulrichs and C. Ciuti. Support by DARPA, the Army Research Office and the Office of Naval Research is gratefully acknowledged.

*Corresponding author.
Electronic address: allen@iquest.ucsb.edu

[1] C. Zener, Proc. R. Soc. London A **145**, 523 (1934).
[2] G. H. Wannier, Phys. Rev. **117**, 432 (1960).
[3] E. E. Mendez, F. Agulló-rueda, and J. M. Hong, Phys. Rev. Lett. **60**, 2426 (1988).
[4] J. Feldmann *et al.*, Phys. Rev. B **46**, 7252 (1992).
[5] C. Waschke *et al.*, Phys. Rev. Lett. **70**, 3319 (1993).
[6] T. Dekorsy, P. Leisching, K. Köhler, and H. Kurz, Phys. Rev. B **50**, 8106 (1994).
[7] Time domain spectroscopy on electrically biased superlattices has been revisited and reinterpreted by Shimada *et al.* by relating transients to the magnitude of the dynamical conductivity that exhibits a resonant peak at the Bloch frequency. Y. Shimada, K. Hirakawa, M. Odnoblioudov, and K. A. Chao, Phys. Rev. Lett. **90**, 046806 (2003).
[8] K. Unterrainer *et al.*, Phys. Rev. Lett. **76**, 2973 (1996).
[9] B. P. Anderson and M. A. Kasevich, Science **282**, 1686 (1998).
[10] M. Ben-Dahan *et al.*, Phys. Rev. Lett. **76**, 4508 (1996).
[11] S. R. Wilkinson *et al.*, Phys. Rev. Lett. **76**, 4512 (1996).
[12] L. Esaki and R. Tsu, IBM J. Res. Dev. **14**, 61 (1970).
[13] S. A. Ktitorov, G. S. Simin, and V. Y. Sindalovski, Fiz. Tverd. Tela **13**, 2230 (1971) [Sov. Phys. Solid State **13**, 1872 (1972)].
[14] S. J. Allen *et al.*, in *Proceedings of the NATO Advanced Research Workshop on Terahertz Sources and Systems* (Kluwer, Dordrecht, 2001), pp. 3–14.
[15] H. Willenberg, G. H. Döhler, and J. Faist, Phys. Rev. B **67**, 085315 (2003).
[16] Measurements show a strong reduction in net loss, but we cannot know if there is net gain unless the system oscillates or exhibits net amplification.
[17] J. Faist *et al.*, Science **264**, 553 (1994).
[18] R. Köhler *et al.*, Nature (London) **417**, 156 (2002).
[19] B. S. Willams *et al.*, Appl. Phys. Lett. **83**, 2124 (2003).
[20] W. Shockley, Bell Syst. Tech. J. **33**, 799 (1954).
[21] H. Kroemer, Proc. IEEE **58**, 1844 (1970).
[22] S. M. Sze, *High-Speed Semiconductor Devices* (Wiley-Interscience, New York, 1990).
[23] A. A Ignatov *et al.*, Sov. Phys. Semicond. **19**, 1345 (1985); K. Hofbeck *et al.*, Phys. Lett. A **218**, 349 (1996).
[24] I.-H. Tan, G. L. Snider, and E. L. Hu, J. Appl. Phys. **68**, 4071 (1990).
[25] This is confirmed by applying double voltage pulses and comparing the *I-V*'s measured with each pulse as the time separation between the two pulses is varied. The bias voltage at which the current starts to rise sharply in the second pulse is critically dependent on the time separation between the pulses.